Atmospheric removal of methane by enhancing the natural hydroxyl radical sink

Atmospheric Removal of Methane by enhancing the natural hydroxyl radical sink

Yuyin Wang[1], Tingzhen Ming[2], Wei Li[1]*, Qingchun Yuan[3], Renaud de Richter[4], Philip Davies[5], Sylvain Caillol[6].

[1] Institute for Materials and Processes, School of Engineering, University of Edinburgh, EH9 3FB, Scotland, UK

[2] School of Civil Engineering and Architecture, Wuhan University of Technology, Wuhan 430070, P. R. China.

[3] Chemical Engineering and Applied Chemistry, Aston University, B4 7ET, the UK

[4] Tour-Solaire.fr, 8 Impasse des Papillons, 34090 Montpellier, France.

[5] School of Engineering, University of Birmingham, Edgbaston, Birmingham, B15 2TT, UK.

[6] Institut Charles Gerhardt CNRS 5253, ENSCM – 34296 Montpellier Cedex 5, France.

* Corresponding author

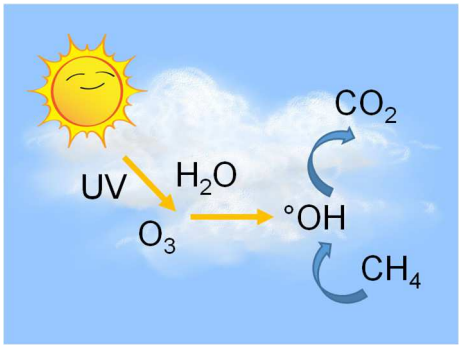

Abstract

According to the latest report from the Intergovernmental Panel on Climate Change (IPCC), currently, global warming due to methane (CH_4) alone is about 0.5°C while due to carbon dioxide (CO_2) alone is about 0.75°C. As CH_4 emissions will continue growing, in order to limit warming to 1.5˚C, some of the most effective strategies are rapidly reducing CH_4 emissions and developing large scale CH_4 removal methods. The aim of this review article is to summarise and propose possible methods for atmospheric CH_4 removal, based on the hydroxyl radical (°OH), which is the principal natural sink of many gases in the atmosphere and on many water surfaces. Inspired by mechanisms of °OH generation in the atmosphere

and observed or predicted enhancement of °OH by climate change and human activities, we proposed several methods to enhance the °OH sink by some physical means using water vapour and artificial UV radiation.

Keywords: hydroxyl radical; natural sink; methane removal; greenhouse gas removal; negative emissions technology; water vapour; UV light

Synopsis: Atmospheric methane concentrations are high and rising. This review article assesses the status and proposes new methods for atmospheric methane removal.

1. Introduction

Methane (CH_4), is a potent greenhouse gas (GHG). For a 100-year time horizon, CH_4 has a global warming potential (GWP) 27-35 times higher than that of carbon dioxide (CO_2). It also has a short residence time in the atmosphere with a GWP 84 times higher than that of CO_2 over 20 years.[1]

Currently, CH_4 contributes 0.5°C warming just next to the highest contribution of 0.75°C from CO_2 [2], as shown in Figure 1A, according to the latest report from the Intergovernmental Panel on Climate Change (IPCC). By the end of the century, in a baseline scenario, the warming due to CH_4 alone can be as high as 0.9°C, ranging from 0.75°C to 1.5°C [3].

The tropospheric CH_4 concentration has grown by nearly 2.6 times over its pre-industrial level and is growing faster and faster in the recent two decades,[1] as shown in Figure 1B. In 2020 and 2021 the annual increases in atmospheric CH_4 (respectively 15.3 ppb and 17 ppb) were the largest annual increases ever recorded since systematic measurements began [4].

CH_4 sources are widely spread from natural sources (e.g. tropical wetlands, thawing permafrost and submarine CH_4-clathrates, lakes and reservoirs) and anthropogenic emissions (e.g. rice paddies, landfills, fossil fuels, livestock, agriculture, wildfires and biomass burning,

hydroelectric installations, as shown in Figure 1C).[5] Global emissions of CH_4 are increasing by shale gas fracking, venting, flaring, fugitive emissions of global gasoline and diesel [6], as well as by leaks in extraction [7], distribution and use [8]. The ones from the fossil fuel industry are 25-40% higher than previous estimates [9].

As CH_4 emissions will continue growing, in order to limit global warming to less than 2°C or below 1.5°C as targeted by the Paris agreement, one of the most effective strategies is rapidly reducing CH_4 emissions. Therefore, a recent United Nations report proposes to reduce by 45% the human-caused CH_4 emissions this decade in order to keep by the end of the century more or less the current warming level due to CH_4 (about 0.5°C) [10]. In November 2021, during the 26th conference of parties COP26 in Glasgow, UK, more than 100 countries signed the Global Methane Pledge committing to reduce 2030 anthropogenic CH_4 emissions by 30% comparatively to 2020 levels [11].

A complementary strategy to CH_4 emission mitigation is CH_4 removal from the atmosphere (i.e. CH_4 remediation).[12] Scientists proposed numerous mitigation methods for CH_4 [13–15], in different sectors such as agricultural soil [16] and animal operations [17]. But remediation proposals for CH_4 already present in the atmosphere are still scarce. [18–22] The main proposals consist of enhancing natural heterogeneous reactions with semi-conductor metal oxides in dusts [23], by photocatalysis [18] or by thermal catalysis [22], as well as by enhancing the Cl atom natural sink of CH_4 [19,24].

The aim of this review is to summarise and propose some possible methods for atmospheric CH_4 removal, based on the hydroxyl radical (°OH), which is the principal natural sink of CH_4 (and also many other gases) in the atmosphere and on many water surfaces.

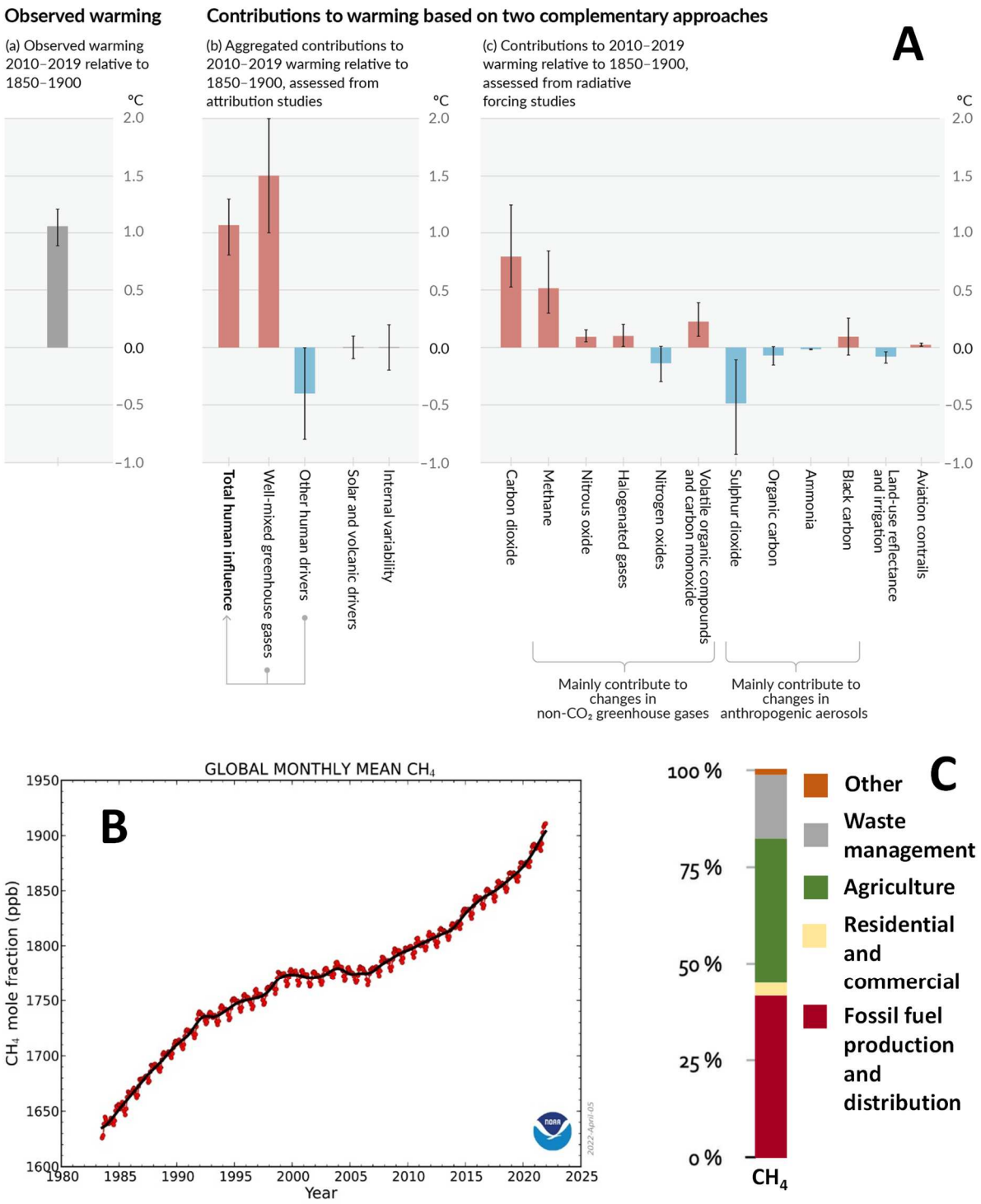

Figure 1: A) Assessed contributions of various warming factors to observed warming in 2010–2019 relative to 1850–1900. Reproduced with permission. [2] Copyright 2021, IPCC. B) Globally-averaged, monthly mean atmospheric CH_4 concentration since 1983. (NOAA Global Monitoring Laboratory). C) Relative sectoral contributions to the anthropogenic emissions of CH_4.[2] Copyright 2021, IPCC.

2. Enhancing the tropospheric °OH sink of CH_4

2.1 Why °OH?

In the troposphere, the major oxidizing agent is the °OH. It is generated naturally and is considered as the detergent of the atmosphere: converting about 3.7 gigatons of trace gases into CO_2 each year [25], including several GHGs and many gases involved in stratospheric ozone (O_3) depletion (man-made hydrofluorocarbons (HFCs) and hydrochlorofluoro-carbons (HCFCs), biogenic chloromethane and bromomethane), volatile organic compounds (VOCs) and urban air pollution. Accordingly, the °OH concentration determines their atmospheric lifetimes.

As shown in Table 1, Prinn et al. [26] summarised some of the principal trace gases in the troposphere, their global emission and the estimated °OH role in their removal (°OH has no effect on CO_2 and N_2O).

Table 1: Global emission of some trace gases in the troposphere and the estimated percent of removal by °OH [26]

Gas	Global emission rate (Tg yr^{-1})	Removal by °OH (%)
CO	2,800	85
CH_4	530	90
C_2H_6	20	90
Isoprene	570	90
Terpenes	140	50
NO_2	150	50
SO_2	300	30
$(CH_3)_2S$	30	90

While the global natural oxidative capacity of the atmosphere seems stable [27], on a wide variety of space and timescales the levels of °OH in the atmosphere don't remain steady but change

rapidly. The °OH sinks increase with pollution emissions of reduced gases (e.g. SO_2, NO, CO). The °OH sources are turned off when UV radiation is absent (night time, polar winter), or decrease by lowering UV radiation (e.g. increasing cloudiness, the recovery of the stratospheric O_3 layer). The °OH sources also decrease for instance by lowering NO_x emissions, decreasing humidity (winter, altitude, droughts, deserted regions…), etc. [26]

2.2 Mechanisms of °OH generation in the atmosphere

The concentrations of °OH depend on numerous factors: concentrations of O_3; relative humidity; temperature; ultraviolet radiation; emissions of VOCs, carbon monoxide (CO), nitrogen oxides (NO_x) [28], and some other factors [29].

An important source for °OH during daytime comes from the UV photolysis of O_3 which generates oxygen and excited atomic oxygen $O(^1D)$, which then reacts with water (H_2O) to produce two OH radicals as in reactions R1 and R2:

$$\text{(R1)} \quad O_3 + h\nu \text{ (UV light)} \rightarrow O_2 + O(^1D)$$

$$\text{(R2)} \quad O(^1D) + H_2O \rightarrow 2\ °OH$$

These reactions show that O_3, H_2O and UV radiation in the wavelength range between 310 nm and 350 nm [30,31] are essential in the troposphere to produce °OH.

As °OH generation is triggered by O_3, UV and humidity, its concentration shows strong day/night cycles and seasonal variations, as well as with height due to decreased H_2O concentration with lower temperatures in altitude. In the tropics, as the humidity is high and the solar radiation is intense, the concentrations of tropospheric °OH are the highest.

UV levels vary mainly with the height of the sun in the sky, the time of day (higher around solar noon), and the time of year (higher in summer), but also with latitude, as the closer to the equator the shorter the distance to travel through the atmosphere and the lower the amount of the UV radiation which is absorbed by the atmosphere. For the same reason, UV levels increase by approximately 10% with every 1 km in altitude.

°OH can also be formed through the reaction between O_3 and some terpenes during the entire 24-hour cycle [32,33], as well as from hydrogen peroxide H_2O_2 by Fenton reaction [34]. The in-situ generation of H_2O_2 can be divided into three categories: chemical, photochemical, and electrochemical pathways that activate O_2 [35]. The photochemical activation is the most likely process that happens in the atmosphere, where the photocatalytic activation of O_2 is usually achieved by photoelectrons from catalysts under light irradiation [36]. The in-situ produced H_2O_2 is catalytically breakdown to generate °OH in this unique Fenton/Fenton-like process [37,38].

3 Observed or predicted enhancement of °OH atmospheric concentration by climate change and human activities

The primary source of tropospheric °OH are reactions R1 and R2 starting with the photo-dissociation of O_3 by solar UV radiation and, in a warmer climate as projected under future global warming characterised by increased amounts of water vapour, the °OH abundance (as well as of other tropospheric oxidants such as HO_2°) is expected to be enhanced in the troposphere. Photolysis rates influence °OH (Reaction R1), and hence variations in the cloud and stratospheric O_3 also have an impact on the concentration of °OH [39].

Lamarque et al. [40], showed that under reduced aerosol emissions, a warmer and moister climate significantly increases global °OH concentration which illustrates the importance of the humidity concentration and distribution. Some studies estimate that in a warmer climate with doubled tropospheric CO_2, the annual global mean °OH concentration would increase by 12.5% [41] or 7% [42].

Regional phenomena should also be noted, such as a ten-fold decrease for °OH in the Tropical West Pacific in relation to the surrounding area and increases in the South Atlantic and East Pacific [43]. Coupled climate chemistry models found that about 85% of CH_4 oxidation by tropospheric °OH occurs between 40°-South and 40°-North [44].

There are not yet publications proposing methods for enhancing the tropospheric °OH sink for CH_4 (as well as of other less concentrated GHGs). But from the above, it can be deduced that

144 if human activities change the humidity levels (e.g. in hot and dry regions with high UV radiation
145 index), the amounts of °OH generated will increase and thus °OH sink for CH_4 will be
146 enhanced.

147 As an example, in some regions of Australia, Saudi Arabia, India or the US, anthropogenic
148 humidity changes already occur, for instance when irrigation for agriculture is made using river
149 flows, fossil groundwater, or sometimes desalinated seawater. Several studies have shown
150 that irrigation can increase relative humidity by 9–20%, and can have significant impacts on
151 local meteorological fields [45]. It is estimated that irrigation in California increases humidity in
152 southwestern U.S. states (Arizona, Colorado, New Mexico, Utah and Wyoming) [46].

153 The modelization made in early 2010's estimates that from 16.7 km^3 of irrigation water used in
154 the summer months over the 52,000 km^2 of irrigated area in Californian Central Valley,
155 evapotranspiration amounts to 14.7 km^3 which benefits the southwestern United States by
156 water vapor export strengthening the regional hydrological cycle. The moisture is blown over
157 the Sierra Nevada, initiating an anthropogenic loop, with a 15% increase in summer
158 precipitation in the other states, and this additional rain in return causes the Colorado River
159 stream flow to experience a 28% boost [46].

160 Due to the global increasing population rates (expected to rise to 9.8 billion by 2050 and
161 11.2 billion in 2100 [47]) significant expansion of irrigated land in developing countries will
162 continue.

163 One possible path to fight global warming is "planting a trillion trees". If this path becomes
164 reality, in order to avoid competition for fertile agricultural land, some arid regions would need
165 to be transformed and that requires irrigation and implies increasing evapotranspiration and
166 more humidity, which in turn will generate more humidity transfer to adjacent regions.

167 Another example of human activity enhanced evaporation in dry regions is the hydroelectric
168 reservoirs. Several dams have been built in dry regions and among them, one of the world's
169 largest reservoirs is Lake Nasser in Egypt, almost 500 km long and with an average width of

about 12 km covering about 6000 km^2 and having a storage capacity of about 162 km^3 of fresh water. The evaporated water loss is estimated to range between 12 and 16 km^3 every year [48–50]. As temperatures and the UV index are high, no doubt that the enhancement of the relative humidity also enhanced the °OH generation.

Human activities can contribute in one more unexpected way. The reasons why the 2020 and 2021 CH_4 concentrations were the highest ever recorded [51] are multifactorial, but one of them is probably due to Covid-19 pandemic lockdowns, as at the global scale the emissions of NOx decreased, leading to a decrease of the levels of tropospheric O_3 [52,53], even if locally in many cities the O_3 burden increased due to other factors [54]. This reduction of NOx emissions and O_3 generation lead to a decrease in the atmospheric CH_4 oxidation due to lower levels of °OH, estimated to be 1.6 to 2% with an atmospheric chemistry transport model [55]. This reduced °OH generation is in turn partially responsible for the record increase of the atmospheric CH_4 concentration in 2020 and 2021.

Last but not least, man-made °OH generators are commercially available and have been proposed for the removal of some pollutants at point sources [56,57]. °OH generators became cheaper with new UV-LEDs which have rather long life-times and whose use has exploded for UV-disinfection or sterilization following the SARS-CoV-2 pandemic. But such systems have not yet been suggested for large scale CH_4 removal.

Table 2 summarises the observed or predicted enhancement of °OH atmospheric concentration by climate change and human activities.

Table 2: Observed or predicted enhancement of °OH atmospheric concentration

By climate change	**Influences**	**Ref.**
Solar UV radiation	Photo-dissociation of O_3	39
Cloud and stratospheric O_3	Photo-dissociation by UV	39
Humidity concentration and distribution	Regional phenomena	40–42
By human activities	**Influences**	

Irrigation for agriculture	Enhanced evaporation	[46]
Hydroelectric reservoirs	Enhanced evaporation	[48–50]
Emissions of NO_x	Changing the lifetime of CH_4	[55]
°OH generators	Direct °OH generation	[56,57]

4 Further enhancement of °OH atmospheric concentration by water vapour

Water vapor is a key link between physical climate and °OH. The previous sections of this paper have focused on the discussion of reasons about more water vapor in hot dry places will generate more °OH. In very dry regions the tropospheric level of °OH is low. By adding humidity to the local atmosphere, which is very sunny and UV rich, °OH will be generated according to reactions R1 and R2.

A device was developed in Israel to generate huge amounts of humidity in very dry regions: it is named the downdraft energy tower (DET). It is a power plant that generates electricity by using sea water and solar energy stored in hot, dry desert air [58]. As demonstrated in Figure 2, the DET [59] includes a high downdraft evaporation tower, pumps, pipes, turbines and water reservoirs. The DET must be located inland, in the driest possible area, because moisture reduces the yield; yet, the DET should not be too distant from the ocean, since seawater is required and piped through ducts to the DET. Then, sea water is pumped to the top of the DET and sprayed with a slew of nebulizers. Water droplets fall and evaporate, creating a downward flow of cold air that is denser than the ambient air. To ensure humidity saturation, the tower is relatively big and tall (usually 400 m in diameter and 1.4 km in height). The strong artificially generated cold wind powers turbines at the base of the tower. Only about a third of the electricity generated is required to pump the seawater to the top of the tower and from the ocean. For this technology, the higher the temperature differential between water and ambient air, the higher the energy efficiency. The energy required is collected from the air, i.e., the ultimate source is the sun. This means that it can be considered as a form of solar power generation [58].

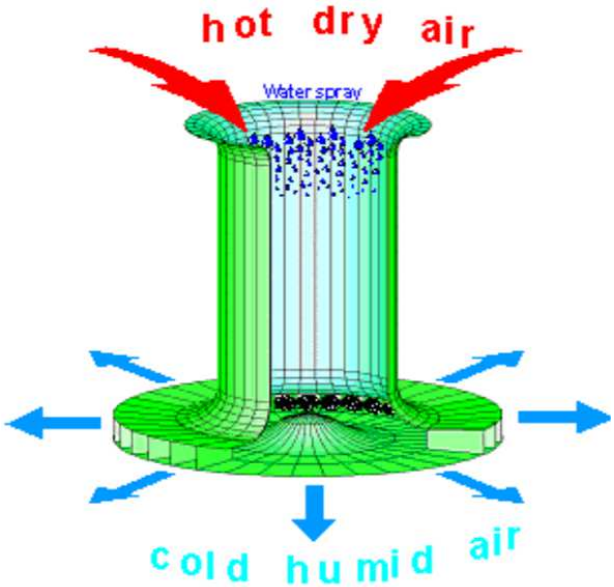

Figure 2. Schematic illustration of the energy tower, Reproduced with permission [60]. Copyright Czisch and Technion - Israel Institute of Technology.

In comparison with many other renewable energy systems, the temporal behavior of the DET is particularly beneficial. As dry air is accessible 24 hours a day, the daily fluctuations are minimal. The ideal areas are along the desert belts' coastlines, where Passat Winds, for example, supply hot dry air. There are no transportation or elevation losses for bringing water to the chimney's foot there. About 41 m^3s^{-1} of water are evaporated, representing 15 g of water per kg of air processed [61] and about 1.3 km^3 per year: ten such downdraft towers evaporate nearly the same quantity of water than due to irrigation in California or to Lake Nasser evaporation losses.

The daily amount of °OH generated by a DET can be calculated via the following equation, based on reaction R1 and R2:

$$N(°OH) = 2N(O_3) = 2 \times N(air) \times c(O_3) = 2 \times c(O_3) \times \frac{Q(air)}{22.4L/mol} = 2 \times c(O_3) \times \frac{tvS}{22.4L/mol}$$

where, $c(O_3)$ means the concentration of O_3 in the atmosphere (approximately 1ppm at 1.4km) ; t represents the time $(24 \times 3600s)$; v is the air velocity at the tower's bottom (17.8 m/s [15]) and S is the bottom surface area of the tower. As a result, it is about 1.724×10^7 mol.

As we mentioned earlier, the DET is a power plant that generates electricity by using sea water and solar energy stored in hot, dry desert air [58]. Herein, the water vapour is generated from this process as a by-product, which does not require additional energy. Take the cooling tower built by Abdelsalam et al. as an example, the tower generates 409 MWh of gross energy annually. 40% of that (164 MWh) is utilised to power the pumps that elevate the water to the top of the chimney. System losses consume 20% of the gross energy (82 MWh). As a result, the net benefit is 40% (164 MWh) of usable energy [63].

5 Further enhancement of °OH atmospheric concentration by artificial UV radiation

The atmospheric concentration of °OH can also be enhanced by artificial UV-B radiation to generate both O_3 (via photolysis of O_2)[64] and °OH in locations or at times where their concentration is low and when the risks are minimal both for fauna and flora.

Several types of UV lamps are commercially available such as conventional ones with Hg vapour inside, economy bulbs (without the coating transforming the UV into visible light), and light emitting diodes (LEDs). Their lifetimes and efficiencies increase in the order cited, while their energy consumptions and prices decrease. The wavelength specificity was generally good and is still improving for both visible LEDs and UV-LEDs, which are more and more used in horticulture (some higher plants and green algae have a UV-B photoreceptor named UV-R8 [65]) and for analytical purposes, for instance, diode array detectors coupled with chromatographic apparatus [66] equip almost all modern laboratory. Selective UV reflecting mirrors [67] allow directing the radiation in the desired direction.

5.1 Safest locations for generating tropospheric O_3 and °OH by artificial UV light

In order not to add to the surface O_3 burden over polluted cities, the UV light generators would be located in unpopulated areas, preferably at sources of CH_4 emissions, such as Siberia, the Arctic, coal mines, open pit mines, regions of shale gas extraction by fracking, rice paddies, wetlands, etc.

Either the UV radiation is directed upwards to the outer space, in order to protect plants and animals from possible damage; or is used in a closed environment such as the ventilation system of a coal mine.

Other possible locations are over the oceans on fixed floating platforms or moving marine vessels in the Southern Oceans far from populated areas.

The main idea is that the O_3 will be generated locally and rapidly consumed to generate °OH and oxidize CH_4 and other VOCs.

5.2 Using balloons, airships, aerostats or flying kites for both holding the UV lamps and power generation

Electrical power generated in altitude, as described in numerous articles [68,69] and patents [70], can be designed to light UV lamps.

Collecting solar and wind energy is ideal in altitude as winds and solar radiation are more regular and intense. Several types of devices (e.g. aerostats, platforms with PV panels [71] and kites with wind turbines [72]) have been proposed for such applications. Several studies show that, compared to a typical ground-based system, locating them in altitude might bring a significant advantage for the electrical power production [73].

The feasibility and viability of such techniques which have been studied are not included in this review article, but as an example: the collection of solar energy at altitudes of 6 to 12 km with the help of a device shown in Figure 3 could produce 4 to 6 times more electricity than on grounds [73]. As a matter of fact, as reaction R1 requires H_2O and O_3 to generate °OH, lower altitudes are necessary. Also, the weight of UV lamps (UV LEDs) needs to be taken into consideration when designing those devices.

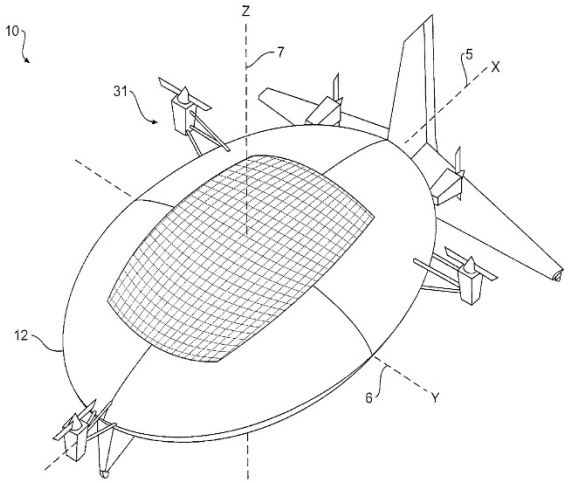

Figure 3: A possible lighter than air platform for solar energy collection, reproduced with permission. [74] Copyright 2014, United States Patent.

5.3 Ocean based platforms, kites or artificial islands for both holding the UV *lamps* and power generation

When the wind is blowing from land to sea, the use of offshore wind turbines is also possible to power UV lamps. Several types of alternative power generating devices are described, such as kite-surf plants [75], sailing wind farms [76], and artificial floating islands or platforms [77] with multiple renewable energy sources including other marine energies.

During peak load, 100% of electricity produced can be sent to the grid. Before and after the peak of consumption, almost all electricity production could be devoted to the UV lamps. At night some base-load electricity production from the grid, or "excess" wind energy which often costs zero or even has a negative price can be used.

The use of batteries to store PV generated electricity for night use is probably not necessary because this will unnecessarily increase the costs of the GGR method proposed. CH_4 is a well-mixed GHG and has many types of natural and anthropogenic sources all over the planet, so any excess of electricity produced in the night or even during the day time could immediately be used for GGR.

6. Further discussions

Limitations in tropospheric O_3 concentrations. In case tropospheric O_3 concentrations become the bottleneck for °OH generation and more tropospheric O_3 is needed, O_3 generation can be considered far from populations in altitude, or over high seas. Because surface O_3 has detrimental effects on vegetation, animals and humans [78]. Another possibility is commercially available °OH generators (described earlier at the end of Section 3) which do not rely on tropospheric O_3 concentrations.

°OH also reacts with other gases and may generate secondary pollutants. Therefore, a rigorous atmospheric chemistry evaluation of rates and mixing is needed for further quantitative analysis of efficiency, costs, environmental and life cycle impacts, etc. This is a knowledge gap in the research field as great diversity exists among different atmospheric chemistry models which predict °OH variability, distribution, and trends. This diversity has been primarily attributed to the following factors: differences in chemical mechanisms that result in differences in the chemical drivers of °OH, differences in meteorology across models that arise either because models produce their own meteorology or are forced by reanalyzed meteorological fields. The quantitative analysis would only be possible once a robust atmospheric model becomes available. Alternatively, some semi-quantitative and scenario-based analyses can be attempted to partially bridge this gap.

Water vapor also has a greenhouse effect and absorbs UV. The average residence time of water vapor in the atmosphere is much shorter than that of CH_4 (4–9 days [79,80]), therefore, if CH_4 oxidation is enhanced, it is expected that the climate benefits should be higher, but this has to be quantified by further atmospheric chemistry modelling, which adds more complexity for the development of atmospheric models. Water vapor and artificial UV rays will not offset each other. Artificial UV is only proposed above oceans, or at altitude in locations that do not require adding additional water vapor. Increasing water vapor using downdraft towers is suggested in hot dry deserts where the natural UV levels are quite high and the use of artificial UV is not required.

Co-benefit of CH_4 removal. Some latest modelling work reveals that CH_4 removal provides great benefits for regional surface O_3 reduction in locations where it has detrimental effects, and thus plays a critical role in improving air quality [81].

Life cycle assessments of all methods proposed. In order to assess if the methods proposed are overall negative emissions, or if the production and deployment of the devices proposed generate more GHGs than they remove, life cycle assessments will be performed in future work. In particular, for devices that only remove CH_4 without any associated co-benefit, the amount of operation time needed to equalize the pollution associated with the manufacture and construction process has to be determined. For devices also producing renewable energy or other co-benefits, more complicated assessments are needed to account for all contributors.

7. Concluding remarks

There are different approaches to develop the much-needed negative emissions technologies. In this review paper, we discussed some strategies to remove atmospheric CH_4 by enhancing the natural °OH sink.

Inspirations can be found in observed or predicted enhancement of °OH atmospheric concentration by climate change and human activities. Change of humidity and introduction of artificial UV radiation are the two main topics here, which we believe deserve more attention from the scientific community to help evaluate their potential risks, impacts, costs and public acceptability.

It is worth pointing out that those strategies may be expensive and have externalities, so careful assessments (e.g. techno-economic analysis, life cycle assessment) will be required to compare the proposed schemes versus CH_4 emission mitigation approaches. We believe that one of the main knowledge gaps for such assessments is the great diversity among different atmospheric chemistry models which predict °OH variability, distribution, and trends.

If the knowledge gap closes and evaluations prove those proposed schemes are viable, together with GHGs mitigation and CO_2 removal, large scale CH_4 removal methods can help win time to fight climate change by slowing down warming and thus meet the targets of the Paris Agreement with limited temperature overshoot.

Acknowledgement

This research was supported by the European Commission H2020 Marie S Curie Research and Innovation Staff Exchange (RISE) award (Grant No. 871998), and the National Key Research and Development Plan (Key Special Project of Inter-governmental National Scientific and Technological Innovation Cooperation, Grant No. 2019YFE0197500).

References

1. NOAA. Earth System Research laboratories. https://www.esrl.noaa.gov/gmd/ccgg/trends_ch4/ (2021).
2. IPCC. Climate Change 2021: The Physical Science Basis. Working Group I contribution to the Sixth Assessment Report of the Intergovernmental Panel on Climate Change. Figure SPM-2. https://www.ipcc.ch/report/ar6/wg1/figures/summary-for-policymakers/.
3. Ocko, I. B. *et al.* Acting rapidly to deploy readily available methane mitigation measures by sector can immediately slow global warming. *Environ. Res. Lett.* **16**, 054042 (2021).
4. NOAA. Increase in atmospheric methane set another record during 2021. https://www.noaa.gov/news-release/increase-in-atmospheric-methane-set-another-record-during-2021 (2022).
5. Saunois, M. *et al.* The Global Methane Budget 2000–2017. *Earth Syst. Sci. Data* **12**, 1561–1623 (2020).
6. Pieprzyk, B. & Hilje, P. R. Influence of methane emissions on the GHG emissions of fossil fuels. *Biofuels, Bioprod. Biorefining* **13**, 535–551 (2019).
7. Pandey, S. *et al.* Satellite observations reveal extreme methane leakage from a natural gas well blowout. *Proc. Natl. Acad. Sci.* **116**, 26376–26381 (2019).
8. Schwietzke, S. *et al.* Upward revision of global fossil fuel methane emissions based on isotope database. *Nature* **538**, 88–91 (2016).
9. Hmiel, B. *et al.* Preindustrial $^{14}CH_4$ indicates greater anthropogenic fossil CH_4 emissions. *Nature* **578**, 409–412 (2020).
10. UNEP. Global Assessment: Urgent steps must be taken to reduce methane emissions

this decade. https://www.unep.org/news-and-stories/press-release/global-assessment-urgent-steps-must-be-taken-reduce-methane (2021).

11. Global Methane Pledge. https://www.globalmethanepledge.org/.

12. Gasser, T., Guivarch, C., Tachiiri, K., Jones, C. D. & Ciais, P. Negative emissions physically needed to keep global warming below 2 °C. *Nat. Commun.* **6**, 7958 (2015).

13. Nisbet, E. G. *et al.* Methane Mitigation: Methods to Reduce Emissions, on the Path to the Paris Agreement. *Rev. Geophys.* **58**, e2019RG000675 (2020).

14. Johannisson, J. & Hiete, M. A Structured Approach for the Mitigation of Natural Methane Emissions—Lessons Learned from Anthropogenic Emissions. *C — J. Carbon Res.* **6**, 24 (2020).

15. Stolaroff, J. K. *et al.* Review of Methane Mitigation Technologies with Application to Rapid Release of Methane from the Arctic. *Environ. Sci. Technol.* **46**, 6455–6469 (2012).

16. Ussiri, D. & Lal, R. *The Role of Nitrous Oxide on Climate Change*. *Soil Emission of Nitrous Oxide and its Mitigation* (Springer Science & Business Media, 2013). doi:10.1007/978-94-007-5364-8_1.

17. Hristov, A. N. *et al.* SPECIAL TOPICS — Mitigation of methane and nitrous oxide emissions from animal operations: I. A review of enteric methane mitigation options1. *J. Anim. Sci.* **91**, 5045–5069 (2013).

18. De_Richter, R., Ming, T., Davies, P., Liu, W. & Caillol, S. Removal of non-CO 2 greenhouse gases by large-scale atmospheric solar photocatalysis. *Prog. Energy Combust. Sci.* **60**, 68–96 (2017).

19. Oeste, F. D., de Richter, R., Ming, T. & Caillol, S. Climate engineering by mimicking natural dust climate control: the iron salt aerosol method. *Earth Syst. Dyn.* **8**, 1–54 (2017).

20. Boucher, O. & Folberth, G. A. New Directions: Atmospheric methane removal as a way to mitigate climate change? *Atmos. Environ.* **44**, 3343–3345 (2010).

21. De_Richter, R. K., Oeste, F. D., Ming, T. & Caillol, S. Iron Salt Aerosol and

Photocatalytic Solar Chimneys: Two innovative breakthrough technologies to remove greenhouse gases. in *Conference: International Conference on Negative CO_2. Emissions 2018: Goteborg, in Sweden 22-24 May 2018.*

22. Jackson, R. B., Solomon, E. I., Canadell, J. G., Cargnello, M. & Field, C. B. Methane removal and atmospheric restoration. *Nat. Sustain.* **2**, 436–438 (2019).

23. George, C., Ammann, M., D'Anna, B., Donaldson, D. J. & Nizkorodov, S. A. Heterogeneous Photochemistry in the Atmosphere. *Chem. Rev.* **115**, 4218–4258 (2015).

24. Ming, T., Richter, R. de, Dietrich Oeste, F., Tulip, R. & Caillol, S. A nature-based negative emissions technology able to remove atmospheric methane and other greenhouse gases. *Atmos. Pollut. Res.* **12**, 101035 (2021).

25. Prinn, R. G. *et al.* Evidence for variability of atmospheric hydroxyl radicals over the past quarter century. *Geophys. Res. Lett.* **32**, L07809-n/a (2005).

26. Prinn, R. G. Ozone, Hydroxyl Radical, and Oxidative Capacity. in *Treatise on Geochemistry* vols 4–9 1–19 (Elsevier, 2003).

27. Rigby, M. *et al.* Role of atmospheric oxidation in recent methane growth. *Proc. Natl. Acad. Sci.* **114**, 5373–5377 (2017).

28. Nicely, J. M. *et al.* A machine learning examination of hydroxyl radical differences among model simulations for CCMI-1. *Atmos. Chem. Phys.* **20**, 1341–1361 (2020).

29. He, J., Naik, V. & Horowitz, L. W. Hydroxyl Radical (OH) Response to Meteorological Forcing and Implication for the Methane Budget. *Geophys. Res. Lett.* **48**, e2021GL094140 (2021).

30. Matsumi, Y. Quantum yields for production of O(^{1}D) in the ultraviolet photolysis of ozone: Recommendation based on evaluation of laboratory data. *J. Geophys. Res.* **107**, ACH 1-1-ACH 1-12 (2002).

31. Hofzumahaus, A. Photolysis frequency of O_3 to O(^{1}D): Measurements and modeling during the International Photolysis Frequency Measurement and Modeling Intercomparison (IPMMI). *J. Geophys. Res.* **109**, D08S90 (2004).

32. Paulson, S. E., Chung, M., Sen, A. D. & Orzechowska, G. Measurement of OH radical formation from the reaction of ozone with several biogenic alkenes. *J. Geophys. Res. Atmos.* **103**, 25533–25539 (1998).

33. Atkinson, R., Aschmann, S. M., Arey, J. & Shorees, B. Formation of OH radicals in the gas phase reactions of O_3 with a series of terpenes. *J. Geophys. Res.* **97**, 6065 (1992).

34. Liu, Y., Zhao, Y. & Wang, J. Fenton/Fenton-like processes with in-situ production of hydrogen peroxide/hydroxyl radical for degradation of emerging contaminants: Advances and prospects. *J. Hazard. Mater.* **404**, 124191 (2021).

35. Pi, L. *et al.* Generation of H_2O_2 by on-site activation of molecular dioxygen for environmental remediation applications: A review. *Chem. Eng. J.* **389**, 123420 (2020).

36. Jiang, Z., Wang, L., Lei, J., Liu, Y. & Zhang, J. Photo-Fenton degradation of phenol by CdS/rGO/Fe2+ at natural pH with in situ-generated H_2O_2. *Appl. Catal. B Environ.* **241**, 367–374 (2019).

37. Bokare, A. D. & Choi, W. Zero-valent aluminum for oxidative degradation of aqueous organic pollutants. *Environ. Sci. Technol.* **43**, 7130–7135 (2009).

38. Su, P. *et al.* Electrochemical catalytic mechanism of N-doped graphene for enhanced H_2O_2 yield and in-situ degradation of organic pollutant. *Appl. Catal. B Environ.* **245**, 583–595 (2019).

39. Stevenson, D. S. *et al.* Trends in global tropospheric hydroxyl radical and methane lifetime since 1850 from AerChemMIP. *Atmos. Chem. Phys.* **20**, 12905–12920 (2020).

40. Lamarque, J.-F. Response of a coupled chemistry-climate model to changes in aerosol emissions: Global impact on the hydrological cycle and the tropospheric burdens of OH, ozone, and NO_x. *Geophys. Res. Lett.* **32**, L16809 (2005).

41. Johnson, C. E., Collins, W. J., Stevenson, D. S. & Derwent, R. G. Relative roles of climate and emissions changes on future tropospheric oxidant concentrations. *J. Geophys. Res. Atmos.* **104**, 18631–18645 (1999).

42. Brasseur, G. P. *et al.* Past and future changes in global tropospheric ozone: Impact on radiative forcing. *Geophys. Res. Lett.* **25**, 3807–3810 (1998).

43. Wolfe, G. M. *et al.* Mapping hydroxyl variability throughout the global remote troposphere via synthesis of airborne and satellite formaldehyde observations. *Proc. Natl. Acad. Sci.* **116**, 11171–11180 (2019).

44. Holmes, C. D., Prather, M. J., Søvde, O. A. & Myhre, G. Future methane, hydroxyl, and their uncertainties: key climate and emission parameters for future predictions. *Atmos. Chem. Phys.* **13**, 285–302 (2013).

45. Sorooshian, S., Li, J., Hsu, K. & Gao, X. How significant is the impact of irrigation on the local hydroclimate in California's Central Valley? Comparison of model results with ground and remote-sensing data. *J. Geophys. Res.* **116**, D06102 (2011).

46. Lo, M. & Famiglietti, J. S. Irrigation in California's Central Valley strengthens the southwestern U.S. water cycle. *Geophys. Res. Lett.* **40**, 301–306 (2013).

47. UN. World population projected to reach 9.8 billion in 2050, and 11.2 billion in 2100. https://www.un.org/development/desa/en/news/population/world-population-prospects-2017.html (2017).

48. Ebaid, H. M. I. & Ismail, S. S. Lake Nasser evaporation reduction study. *J. Adv. Res.* **1**, 315–322 (2010).

49. Abou El-Magd, I. H. & Ali, E. M. Estimation of the evaporative losses from Lake Nasser, Egypt using optical satellite imagery. *Int. J. Digit. Earth* **5**, 133–146 (2012).

50. Hassan, A., Ismail, S. S., Elmoustafa, A. & Khalaf, S. Evaluating evaporation rate from high Aswan Dam Reservoir using RS and GIS techniques. *Egypt. J. Remote Sens. Sp. Sci.* **21**, 285–293 (2018).

51. NOAA. Despite pandemic shutdowns, carbon dioxide and methane surged in 2020. https://research.noaa.gov/article/ArtMID/587/ArticleID/2742/Despite-pandemic-shutdowns-carbon-dioxide-and-methane-surged-in-2020) (2021).

52. Steinbrecht, W. *et al.* COVID-19 Crisis Reduces Free Tropospheric Ozone Across the Northern Hemisphere. *Geophys. Res. Lett.* **48**, e2020GL091987 (2021).

53. Miyazaki, K. *et al.* Global tropospheric ozone responses to reduced NO_x emissions linked to the COVID-19 worldwide lockdowns. *Sci. Adv.* **7**, eabf7460 (2021).

492 54. Sicard, P. *et al.* Amplified ozone pollution in cities during the COVID-19 lockdown. *Sci.*
493 *Total Environ.* **735**, 139542 (2020).
494 55. Stevenson, D., Derwent, R., Wild, O. & Collins, W. COVID-19 lockdown NO_x emission
495 reductions can explain most of the coincident increase in global atmospheric methane.
496 *Atmos. Chem. Phys. Discuss.* **2021**, 1–8 (2021).
497 56. Morneault, G. J. E. US2013004381 (A1) - Hydroxyl Generator. (2013).
498 57. Engstrom G Eric. US2016325004 (A1) - Hydroxyl Generation and/or Ozone Reduction
499 System and Method. (2016).
500 58. Ming, T., De_Richter, R., Liu, W. & Caillol, S. Fighting global warming by climate
501 engineering: Is the Earth radiation management and the solar radiation management
502 any option for fighting climate change? *Renew. Sustain. Energy Rev.* **31**, 792–834
503 (2014).
504 59. Omer, E., Guetta, R., Ioslovich, I., Gutman, P.-O. & Borshchevsky, M. Optimal Design
505 of an “Energy Tower” Power Plant. *IEEE Trans. Energy Convers.* **23**, 215–225 (2008).
506 60. Altman, T., Zaslavsky, D., Guetta, R. & Czisch, G. Evaluation of the potential of
507 electricity and desalinated water supply by using technology of " Energy Towers " for
508 Australia and America. *Energy* (2005).
509 61. Energy tower (downdraft). 1–4 https://en.wikipedia.org/wiki/Energy_tower_(downdraft).
510 62. Altmann, T., Carmel, Y., Guetta, R., Zaslavsky, D. & Doytsher, Y. Assessment of an
511 “Energy Tower” potential in Australia using a mathematical model and GIS. *Sol. Energy*
512 **78**, 799–808 (2005).
513 63. Abdelsalam, E. *et al.* Performance analysis of hybrid solar chimney–power plant for
514 power production and seawater desalination: A sustainable approach. *Int. J. Energy*
515 *Res.* **45**, 17327–17341 (2021).
516 64. Claus, H. Ozone Generation by Ultraviolet Lamps †. *Photochem. Photobiol.* **97**, 471–
517 476 (2021).
518 65. Fernández, M. B., Tossi, V., Lamattina, L. & Cassia, R. A Comprehensive Phylogeny
519 Reveals Functional Conservation of the UV-B Photoreceptor UVR8 from Green Algae

to Higher Plants. *Front. Plant Sci.* **7**, 1698 (2016).

66. Bomastyk, B., Petrovic, I. & Hauser, P. C. Absorbance detector for high-performance liquid chromatography based on light-emitting diodes for the deep-ultraviolet range. *J. Chromatogr. A* **1218**, 3750–3756 (2011).

67. Smirnov, J. R. C., Calvo, M. E. & Míguez, H. Selective UV Reflecting Mirrors Based on Nanoparticle Multilayers. *Adv. Funct. Mater.* **23**, 2805–2811 (2013).

68. Aglietti, G. S., Redi, S., Tatnall, A. R. & Markvart, T. Harnessing High-Altitude Solar Power. *IEEE Trans. Energy Convers.* **24**, 442–451 (2009).

69. Fagiano, L., Milanese, M. & Piga, D. High-Altitude Wind Power Generation. *IEEE Trans. Energy Convers.* **25**, 168–180 (2010).

70. Shepard, D. H. Power generation from high altitude winds. Patent US 4,659,940 (1987).

71. Aglietti, G. S., Markvart, T., Tatnall, A. R. & Walker, S. J. Solar power generation using high altitude platforms feasibility and viability. *Prog. Photovoltaics Res. Appl.* **16**, 349–359 (2008).

72. Canale, M., Fagiano, L. & Milanese, M. High Altitude Wind Energy Generation Using Controlled Power Kites. *IEEE Trans. Control Syst. Technol.* **18**, 279–293 (2010).

73. Aglietti, G. S., Redi, S., Tatnall, A. R. & Markvart, T. High altitude electrical power generation. *WSEAS Trans. Environ. Dev.* **4**, 1067–1077 (2008).

74. Goelet, J. System and method for solar-powered airship. Patent US 8,894,002 (2014).

75. Ahrens, U., Pieper, B. & Töpfer, C. Combining Kites and Rail Technology into a Traction-Based Airborne Wind Energy Plant. in *Airborne Wind Energy* 437–441 (Springer Berlin Heidelberg, 2013). doi:10.1007/978-3-642-39965-7_25.

76. Tsujimoto, M. *et al.* Optimum routing of a sailing wind farm. *J. Mar. Sci. Technol.* **14**, 89–103 (2009).

77. Yeh, N., Yeh, P. & Chang, Y.-H. Artificial floating islands for environmental improvement. *Renew. Sustain. Energy Rev.* **47**, 616–622 (2015).

78. Griffiths, P. T. *et al.* Tropospheric ozone in CMIP6 simulations. *Atmos. Chem. Phys.* **21**, 4187–4218 (2021).

79. van der Ent, R. J. & Tuinenburg, O. A. The residence time of water in the atmosphere revisited. *Hydrol. Earth Syst. Sci.* **21**, 779–790 (2017).

80. Läderach, A. & Sodemann, H. A revised picture of the atmospheric moisture residence time. *Geophys. Res. Lett.* **43**, 924–933 (2016).

81. Abernethy, S., O'Connor, F. M., Jones, C. D. & Jackson, R. B. Methane removal and the proportional reductions in surface temperature and ozone. *Philos. Trans. R. Soc. A Math. Phys. Eng. Sci.* **379**, 20210104 (2021).